

Pumped current and voltage for an adiabatic quantum pump

M. L. Polianski and P. W. Brouwer

Laboratory of Atomic and Solid State Physics, Cornell University, Ithaca, NY 14853-2501

October 27, 2018

We consider adiabatic pumping of electrons through a quantum dot. There are two ways to operate the pump: to create a dc current \bar{I} or to create a dc voltage \bar{V} . We demonstrate that, for very slow pumping, \bar{I} and \bar{V} are not simply related via the dc conductance G as $\bar{I} = \bar{V}G$. For the case of a chaotic quantum dot, we consider the statistical distribution of $\bar{V}G - \bar{I}$. Results are presented for the limiting cases of a dot with single channel and with multichannel point contacts.

PACS numbers: 73.23.-b, 72.10.Bg

I. INTRODUCTION

An electron pump is a device that converts a periodic variation of its characteristics into a time-independent electric current.¹ Such characteristics can be “macroscopic”, like the charge on the device or the conductance of point contacts, or “microscopic”, such as the location of a scatterer or the magnetic flux threading the sample. When there are two characteristics of the device that can be varied harmonically with a frequency ω and phase difference ϕ , pumping of electrons already occurs in the adiabatic limit $\omega \rightarrow 0$. In that case the pumped current is proportional to $\omega \sin \phi$, and changes sign when the phase relationship between the parameters is reversed. Adiabatic electron pumps have been realized experimentally in (arrays of) Coulomb blockaded quantum dots, using the voltages on plunger gates, and/or the transparencies of the contacts as pumping parameters.²⁻⁴

In this paper, we consider an adiabatic electron pump that consist of a semiconductor quantum dot coupled to two electron reservoirs by means of ballistic point contacts.⁵ Variation of two gate voltages allow for small changes of the shape of the dot, and thus for the flow of a dc current. Following a proposal by Spivak *et al.*,⁶ such a device has been built and investigated by Switkes *et al.*⁷ The device of Ref. 7 is referred to as an “adiabatic quantum pump”, because the variation of the gate voltages predominantly affects the quantum interference of the electrons in the quantum dot, not their classical trajectories. An important property of the quantum dot used in the experiment of Ref. 7 is that its classical dynamics is chaotic. As a result, the magnitude and the sign of the expected pumped current \bar{I} are subject to mesoscopic fluctuations. Since these fluctuations are large, the mean $\langle \bar{I} \rangle$ and variance $\langle \bar{I}^2 \rangle$ are insufficient to describe the ensemble, and one needs to know the entire probability distribution $P(\bar{I})$.

Theoretical analysis has focused on the dc current \bar{I} pumped through the dot,⁸⁻¹³

$$\bar{I} = \frac{1}{T} \int_0^T dt I(t), \quad (1)$$

$T = 2\pi/\omega$ being the period of the pumping cycle. However, experimentally, the preferred measurement is that of the dc voltage \bar{V} that the electron pump generates,⁷

$$\bar{V} = \frac{1}{T} \int_0^T dt V(t). \quad (2)$$

Naively, one might expect that, for small pumping amplitudes, \bar{I} and \bar{V} are related via the dot’s conductance G as $\bar{I} = \bar{V}G$. However, as we show in this paper, this naive “Ohm’s law” is not always true, depending on whether the pumping frequency ω is small or large compared to the charge-relaxation rate γ of the reservoirs. (For adiabatic pumping, ω must always be small compared to the charge relaxation rate of the quantum dot.) For $\omega \ll \gamma$ and if the number N of propagating channels in the point contacts between the quantum dot and the electron reservoirs is small, the pumped current \bar{I} and the difference $\bar{D} = \bar{V}G - \bar{I}$ can actually be of comparable magnitude.

A qualitative explanation why the pumped voltage and current are not related via the simple relation $\bar{V}G - \bar{I}$ in the limit $\omega \ll \gamma$ follows from the observation that both the pumped current and the pumped voltage have dc and ac components. For slow pumping, the electron pump generates a bias voltage that counteracts both the dc and ac currents generated in the dot. Since the conductance G itself also varies in time, $V_{ac}G$ has a dc component. It is this additional rectified dc component of the current that is responsible for the difference between $\bar{V}G$ and \bar{I} for an adiabatic electron pump. When pumping is faster than the charge relaxation rate of the reservoirs, no ac bias voltage is generated to balance the ac current, and the difference between $\bar{V}G$ and \bar{I} disappears.

The purpose of this paper is to find the distribution of the difference $\bar{V}G - \bar{I}$ between pumped current and pumped voltage for adiabatic pumping of electrons through a chaotic quantum dot and to compare it to the distributions of \bar{I} and \bar{V} . For a chaotic dot, these distributions have a universal form, independent of details of the pumping mechanism or the shape of the quantum dot. In section II we use the scattering approach to present a quantitative theory for the pumped voltage \bar{V} ,

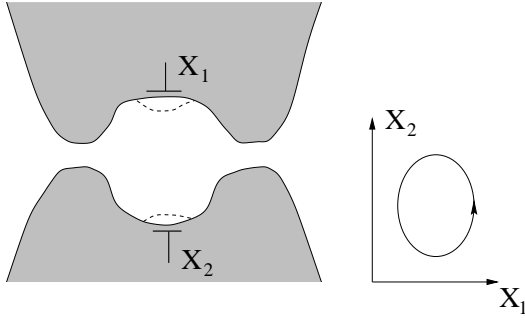


FIG. 1. Schematic of a chaotic quantum dot whose shape can be changed by varying gate voltages X_1 and X_2 (left). In one cycle X_1 and X_2 trace out a contour in (X_1, X_2) space (right).

and the difference $\bar{D} = \bar{V}G - \bar{I}$. In section III we then evaluate the distribution of $\bar{V}G - \bar{I}$ for an ensemble of chaotic quantum dots, using random matrix theory. We conclude in Sec. IV.

II. PUMPED CURRENT AND VOLTAGE

We consider a quantum dot coupled to two electron reservoirs via point contacts, see Fig. 1. The shape of the quantum dot is varied periodically by variation of two gate voltages, represented by dimensionless parameters X_1 and X_2 . Alternatively, X_1 or X_2 can represent the value of an applied magnetic field, or any other parameter that characterizes the quantum dot.

As discussed in the introduction, the electron pump can be characterized experimentally via a direct measurement of the pumped current, or via a measurement of the voltage $V(t)$ between the two reservoirs generated as a result of the pumping of charge through the quantum dot. A formula for the dc current has been derived in Refs. 8,9. To derive a formula for the dc voltage \bar{V} , we introduce a simple model for the quantum dot and the two electron reservoirs, see Fig. 2. The dot and the reservoirs 1, 2 are connected to a screening gate via capacitances C and C_1, C_2 . Following Refs. 14,15, we introduce the emissivity $e\delta q(m)/\delta X_j$, which is the charge that exits the dot through point contact m ($m = 1, 2$) when the parameter X_j ($j = 1, 2$) is changed adiabatically by an amount δX_j . Then the total current flowing through contacts 1 and 2 reads

$$I_1(t) = e \sum_{i=1}^2 \frac{\delta q(1)}{\delta X_i} \frac{dX_i}{dt} + [V_1(t) - V_2(t)]G, \quad (3a)$$

$$I_2(t) = e \sum_{i=1}^2 \frac{\delta q(2)}{\delta X_i} \frac{dX_i}{dt} + [V_2(t) - V_1(t)]G, \quad (3b)$$

where G is the dc conductance of the quantum dot. Here we assume that all variations are made slowly on the scale of the dwell time of the quantum dot.

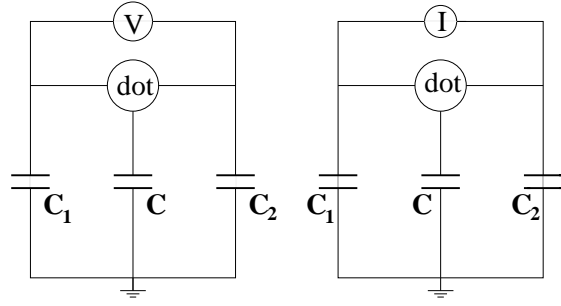


FIG. 2. Equivalent circuit for a measurement of the pumped voltage through the dot (left) and of the pumped current (right). C_i and C are geometrical capacitances of the i -th reservoir and the dot.

When current is measured, the voltages of the two reservoirs are equal, $V_1(t) = V_2(t)$. Hence the dc current \bar{I} can be found from integration of Eq. (3a) or (3b).⁸ Using Stokes' theorem, \bar{I} can be rewritten as an integral over the surface area S enclosed by the contour of the parameters X_1 and X_2 in the (X_1, X_2) plane,

$$\bar{I} = \frac{e\omega}{2\pi} \int dX_1 dX_2 \bar{i}(X_1, X_2), \quad (4a)$$

where

$$\begin{aligned} \bar{i} &= \frac{\partial}{\partial X_2} \frac{\partial q(1)}{\partial X_1} - \frac{\partial}{\partial X_1} \frac{\partial q(1)}{\partial X_2} \\ &= -\frac{\partial}{\partial X_2} \frac{\partial q(2)}{\partial X_1} + \frac{\partial}{\partial X_1} \frac{\partial q(2)}{\partial X_2}. \end{aligned} \quad (4b)$$

When voltage is measured, the result depends on whether variation of the parameters X_1 and X_2 is fast or slow compared to the charge relaxation rates $\gamma_{1,2} \sim G/C_{1,2}$ of the reservoirs. If the variation is fast compared to $\gamma_{1,2}$ (but still slow compared to the charge relaxation rate of the quantum dot), the voltage difference $V_1 - V_2$ is essentially time independent and takes the value

$$\bar{V} = \bar{I}/\bar{G}, \quad (5)$$

where \bar{G} is the conductance averaged over one cycle,

$$\bar{G} = \frac{1}{T} \int_0^T dt G(X_1(t), X_2(t)). \quad (6)$$

In the opposite limit $\omega \ll \gamma_{1,2}$, which is the case we'll consider in the remainder of the paper, one has $I_1(t) = \eta I_2(t)$, where $\eta = C_1/C_2$ is a numerical coefficient describing the capacitive division between the two reservoirs. Combining this with Eq. (3), we find

$$V_1(t) - V_2(t) = \frac{e}{G(1+\eta)} \sum_{i=1}^2 \left(\frac{\delta q(1)}{\delta X_i} \frac{dX_i}{dt} - \eta \frac{\delta q(2)}{\delta X_i} \frac{dX_i}{dt} \right) \quad (7)$$

The dc voltage \bar{V} is then found by integration over the period T , with the result

$$\bar{V} = \frac{h\omega}{4\pi e} \int dX_1 dX_2 \bar{v}(X_1, X_2), \quad (8a)$$

$$\bar{v} = \frac{1}{1+\eta} \left[\frac{\partial}{\partial X_2} \left(\frac{1}{g} \frac{\partial q(1)}{\partial X_1} \right) - \frac{\partial}{\partial X_1} \left(\frac{1}{g} \frac{\partial q(1)}{\partial X_2} \right) \right] - \frac{\eta}{1+\eta} \left[\frac{\partial}{\partial X_2} \left(\frac{1}{g} \frac{\partial q(2)}{\partial X_1} \right) - \frac{\partial}{\partial X_1} \left(\frac{1}{g} \frac{\partial q(2)}{\partial X_2} \right) \right], \quad (8b)$$

where $g = hG/2e^2$ is the dimensionless conductance. For small harmonic variations of the parameters, $X_1(t) = \delta X_1 \cos(\omega t)$ and $X_2(t) = \delta X_2 \cos(\omega t + \phi)$, the integrations are trivial, and one finds

$$\bar{I} = \frac{1}{2} e\omega \delta X_1 \delta X_2 \bar{i} \sin \phi \quad (9)$$

for the pumped current, and

$$\bar{V} = \frac{h\omega}{4e} \delta X_1 \delta X_2 \bar{v} \sin \phi \quad (10)$$

for the pumped voltage.

If the conductance G were constant in a cycle, i.e., G would not depend on X_1 and X_2 , Eqs. (4b) and (8b)–(10) give the identity $\bar{V}G = \bar{I}$: the pumped current measured at zero bias and the pumped voltage measured at zero current are related by Ohm's law. However, in general G does depend on X_1 and X_2 , and this ‘‘Ohm's law’’ does not hold. The deviation is described by the difference

$$\bar{D} = \bar{V}G - \bar{I}. \quad (11)$$

For small δX_1 and δX_2 , we find from Eqs. (4b), (8b),

$$\bar{D} = \frac{1}{2} e\omega \delta X_1 \delta X_2 \bar{d} \sin \phi, \quad (12a)$$

$$\bar{d} = \frac{1}{1+\eta} \left[\frac{1}{g} \frac{\partial g}{\partial X_1} \frac{\partial q(1)}{\partial X_2} - \frac{1}{g} \frac{\partial g}{\partial X_2} \frac{\partial q(1)}{\partial X_1} \right] - \frac{\eta}{1+\eta} \left[\frac{1}{g} \frac{\partial g}{\partial X_1} \frac{\partial q(2)}{\partial X_2} - \frac{1}{g} \frac{\partial g}{\partial X_2} \frac{\partial q(2)}{\partial X_1} \right]. \quad (12b)$$

The derivatives to X_1 and X_2 appearing in the above formulae are derivatives taken at constant values of the electro-chemical potential μ of the reservoirs. These are not necessarily equal to derivatives taken at a constant value of the (self-consistent¹⁶) electrostatic potential V_{sc} inside the quantum dot. Changes of V_{sc} occur in a pumping cycle, because the total charge on the dot may vary during the pumping cycle. For technical reasons, it is preferred to treat V_{sc} , or, equivalently, the kinetic energy $E = \mu - V_{sc}$, as an independent parameter, and to take derivatives at constant E . The above equations for pumped voltage and current can be rewritten using derivatives at constant E if we substitute the parametric derivatives $\partial/\partial X_1$ and $\partial/\partial X_2$ in Eqs. (4b), (8b), and (12b) by^{14,15}

$$\left. \frac{\partial}{\partial X} \right|_{\mu} \rightarrow \left. \frac{\partial}{\partial X} \right|_E + \frac{\partial E}{\partial X} \frac{\partial}{\partial E}, \quad (13a)$$

$$\frac{\partial E}{\partial X_i} = - \frac{\partial q / \partial X_i}{C/2e^2 + \partial q / \partial E}. \quad (13b)$$

Here C is the capacitance of the quantum dot. In Eq. (13a), we abbreviated

$$\frac{\partial q}{\partial X_j} = \frac{\partial q(1)}{\partial X_j} + \frac{\partial q(2)}{\partial X_j}. \quad (14)$$

For a realistic quantum dot, the charging energy e^2/C is much larger than the mean level spacing Δ . In that limit, one finds that the dot charge remains constant during the pumping cycle, $I_1(t) = -I_2(t)$ for all time. As a consequence, the pumped voltage \bar{V} and the difference $\bar{D} = \bar{V}G - \bar{I}$ lose their dependence on the capacitive division η .

In the absence of inelastic processes and for low temperatures (temperature T below the mean level spacing Δ in the quantum dot), the emissivities $\partial q(m)/\partial X_j$ and the conductance G can be expressed in terms of the scattering matrix S of the quantum dot and its derivatives to X_1 , X_2 , and E . The matrix S has dimension $2N$, where N is the number of propagating channels in each point contact; it is unitary (unitary symmetric) in the presence (absence) of a time-reversal symmetry breaking magnetic field. The derivatives of S are parameterized via hermitian matrices R , R_j , defined as¹⁹

$$R = -i \frac{\Delta}{2\pi} \frac{\partial S}{\partial E} S^\dagger, \quad R_j = -i \frac{\partial S}{\partial X_j} S^\dagger.$$

Then the emissivities $\partial q(m)/\partial E$, $\partial q(m)/\partial X$, $m = 1, 2$, are given by¹⁵

$$\frac{\partial q(m)}{\partial E} = \frac{1}{\Delta} \text{Re tr } P_m R, \quad (15a)$$

$$\frac{\partial q(m)}{\partial X_j} = \frac{1}{2\pi} \text{Re tr } P_m R_j. \quad (15b)$$

Here $P_1 = 1 - P_2$ is a diagonal matrix with elements $(P_1)_{jj} = 1$ if $j \leq m$ and zero otherwise. The dc conductance g is given by the Landauer formula,

$$g = \text{tr } S^\dagger P_1 S P_2. \quad (16)$$

In the next section, we shall study the distribution of the dimensionless difference $\bar{d} = \bar{v}g - \bar{i}$ for the case of a chaotic quantum dot.

III. DISTRIBUTION OF $\bar{D} = \bar{V}G - \bar{I}$

For an ensemble of chaotic quantum dots, the statistical distribution of the scattering matrix and its derivatives is known from the literature.¹⁸ It takes its simplest form when the derivative of S is not parameterized by the matrices R_j , R , but by the symmetrized derivatives Q , Q_j ,

$$Q = S^{-1/2} R S^{1/2}, \quad Q_j = S^{-1/2} R_j S^{1/2}.$$

In the presence of time-reversal symmetry (labeled by the Dyson parameter $\beta = 1$), the matrices Q , Q_1 , and

Q_2 are real symmetric. When time-reversal symmetry is broken by a magnetic field ($\beta = 2$), Q , and Q_1 , and Q_2 are hermitian. For ideal contacts, the joint distribution $P(S, Q, Q_1, Q_2)$ reads¹⁸

$$P \propto \left(1 + \frac{2e^2}{C\Delta} \text{tr} Q\right) (\det Q)^{-N/2 - 2(\beta N + 2 - \beta)} \\ \times \exp\left[-\frac{\beta}{2} \text{tr}(Q^{-1})\right] \Theta(Q) \\ \times \exp\left[-\frac{\beta}{16} \text{tr}\left((Q^{-1}Q_1)^2 + (Q^{-1}Q_2)^2\right)\right], \quad (17)$$

where $\Theta(Q) = 1$ if all eigenvalues of Q are positive and $\Theta(Q) = 0$ otherwise. The capacitance C appears in the distribution because the ensemble is obtained by sweeping an external gate voltage, not the self-consistent energy E .¹⁷

To find the distribution $P(\bar{d})$, we first integrate over Q_1 and Q_2 at fixed S and Q , and then over S and Q . The first integration can be done analytically, since, for fixed Q , Q_1 and Q_2 are Gaussian random matrices, see Eq. (17). The result of this integration takes a simple form,

$$P(\bar{d}) = \left\langle \frac{1}{2\sigma} e^{-|\bar{d}|/\sigma} \right\rangle_{S, Q}, \quad (18)$$

where the brackets indicate the average over S and Q that remains to be done. In equation (18) σ is positive function of S and Q , given by

$$\sigma^2 = \left(\frac{16}{\beta g}\right)^2 \left([\text{tr} A^2 + \frac{\delta_{\beta,1}}{2} \text{tr}(PRSPR^T S^\dagger - PRPR)] \text{tr} B^2 - (\text{tr} AB)^2 \right), \quad (19)$$

where we abbreviated

$$A = R \left(P - \frac{\text{tr} PR}{C\Delta/2e^2 + \text{tr} R} \right), \\ B = R \left(\Lambda - \frac{\text{tr} \Lambda R}{C\Delta/2e^2 + \text{tr} R} \right),$$

and $P = (P_1 - \eta P_2)/(1 + \eta)$, $\Lambda = i(P_1 S P_2 S^\dagger - S P_2 S^\dagger P_1)$.

For the remaining integrations over S and Q we consider two limiting cases: multichannel point contacts ($N \gg 1$) and single channel point contacts ($N = 1$).

A. Single-channel contacts

For $N = 1$ the remaining number of variables is small, and can be integrated over numerically, using the distribution (17). Results for the (physically relevant) limit $C\Delta \ll e^2$ are shown in Fig. 3. In this limit, the distribution $P(\bar{d})$ does not depend on the capacitive division η between the reservoirs. The results for larger values of

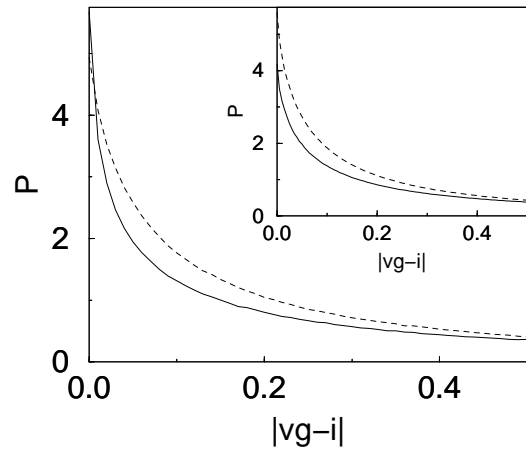


FIG. 3. Distribution of the normalized difference $\bar{d} = \bar{v}g - \bar{i}$ between pumped voltage \bar{v} and pumped current \bar{i} for single-channel point contacts, for the physically relevant limit $C\Delta \ll e^2$ (main figure). The opposite limit $C\Delta \gg e^2$ is shown in the inset for the case $\eta = 0$. Presence (absence) of time-reversal symmetry $\beta = 1$ ($\beta = 2$) is shown solid (dashed).

C are not very different from those shown in Fig. 3. This is illustrated in the inset of Fig. 3, where we have shown the distribution $P(\bar{d})$ for the case of large capacitance $C\Delta \gg e^2$ and asymmetric reservoirs (capacitive division $\eta = 0$). For \bar{d} close to zero, the distribution shows a cusp with a logarithmically divergent derivative at $\bar{d} = 0$. For $\bar{d} \gg 1$, the distribution $P(\bar{d})$ has power-law tails. For $C\Delta \ll e^2$ these are²¹

$$P(\bar{d}) \propto \begin{cases} \bar{d}^{-3}, & \beta = 1, \\ \bar{d}^{-3} \log \bar{d}, & \beta = 2. \end{cases} \quad (20)$$

The tails of the distribution correspond to samples with an anomalously large eigenvalue of Q , corresponding to an anomalously large dwell time τ_D :¹⁹ a value of \bar{d} in the tail of the contribution typically corresponds to a dwell time $\tau_D \sim \tau_H \bar{d}^{2/\beta}$, $\tau_H = \hbar/\Delta$ being the Heisenberg time. Since configurations with anomalously large dwell times are more sensitive to dephasing or thermal smearing, such perturbations will truncate the tails for $\bar{d} \gtrsim (\tau_\phi/\tau_H)^{\beta/2}$ or $\bar{d} \gtrsim (\tau_H T)^{-\beta/2}$.

For comparison, we have also calculated the distribution of the pumped current \bar{i} and voltage \bar{v} . For single-channel contacts, the distribution again takes the form (18), with σ replaced by σ_i and σ_v , respectively. Expressions for σ_i and σ_v can be found in the appendix. The resulting distributions are shown in Fig. 4. (The distribution of the current was calculated previously in Ref. 8.) The main conclusion upon comparison of Figs. 3 and 4 is that, for single-channel point contacts, the distributions of \bar{i} and of $\bar{d} = \bar{v}g - \bar{i}$ have comparable widths. Hence, for $N = 1$, deviations from ‘‘Ohm’s law’’, as characterized by $\bar{d} = \bar{v}g - \bar{i}$ are of the same order as the pumped current \bar{i} itself.

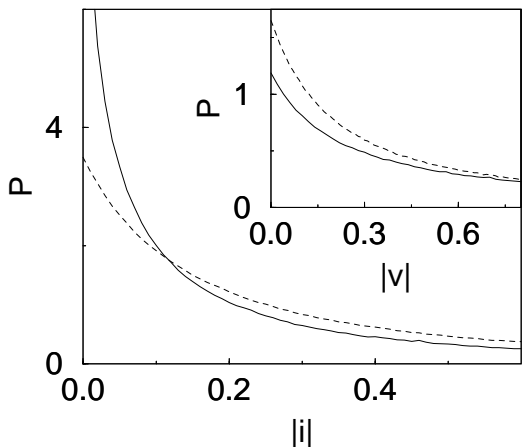


FIG. 4. Distribution of normalized pumped current \bar{i} and (inset) voltage \bar{v} for single-channel contacts. Presence (absence) of time-reversal symmetry $\beta = 1$ ($\beta = 2$) is shown solid (dashed).

B. Multi-channel contacts

The distribution of \bar{d} in the limit $N \gg 1$ can be directly obtained from Eq. (18). The integration over the unitary matrix U of eigenvectors of R and over the scattering matrix S is performed using the method of Ref. 20. For the remaining integration over the eigenvalues $\tau_i, i = 1, \dots, 2N$, of the matrix R it is sufficient to know their density,¹⁸

$$\rho(\tau) = \sum_{j=1}^{2N} \langle \delta(\tau_j - \tau) \rangle = \frac{N}{\pi\tau^2} \sqrt{(\tau_+ - \tau)(\tau - \tau_-)}, \quad (21)$$

where $\tau_{\pm} = (3 \pm \sqrt{8})/2N$. This gives the result

$$\langle \sigma^2 \rangle = \frac{4}{\beta N^4} \left[1 + \frac{4}{\beta} \left(\frac{1-\eta}{1+\eta} \right)^2 \left(\frac{\Delta}{\Delta + 2e^2/C} \right)^2 \right]. \quad (22)$$

Calculation of higher moments of σ shows that fluctuations of σ are small compared to the average as $N \rightarrow \infty$. Hence, we can conclude that the distribution of \bar{d} in multi-channel limit is of the Poissonian form (18), with σ^2 given by Eq. (22).

This is to be contrasted with the distribution of the pumped current \bar{i} , which is Gaussian for large N , with zero mean and with root mean square^{8,10}

$$\langle \bar{i}^2 \rangle^{1/2} = \frac{1}{\pi N}. \quad (23)$$

Hence we conclude that, for large N , typically \bar{d} is a factor $\sim N$ smaller than the pumped current, and can be neglected in a measurement. Hence, in the limit $N \rightarrow \infty$ the expectation of ‘‘Ohm’s law’’ $\bar{v}g = \bar{i}$ holds, and one readily concludes that the pumped voltage \bar{v} has a Gaussian distribution with zero mean and with root mean square

$$\langle \bar{v}^2 \rangle^{1/2} = \frac{2}{\pi N^2}. \quad (24)$$

IV. CONCLUSION

In summary, for adiabatic pumping of electrons through a chaotic quantum dot, we have derived expressions of the pumped current \bar{I} (in case of a current measurement) or the pumped voltage \bar{V} (in case of a voltage measurement) in terms of the scattering matrix of the quantum dot. Pumped current and voltage are not simply related by the dot’s conductance G . We have calculated the distribution of the difference $\bar{V}G - \bar{I}$ for small pumping amplitudes, which is universal for a chaotic quantum dot. If the number N of propagating channels in the contacts between the quantum dot and the reservoirs is one, \bar{I} and $\bar{V}G - \bar{I}$ can be of the same size; if $N \gg 1$, $\bar{V}G - \bar{I}$ is typically a factor N smaller than \bar{I} . Our results are valid in the limit of slow pumping, where the pumping frequency ω is much smaller than the charge relaxation rate γ of the reservoirs. If $\omega \gg \gamma$, the difference $\bar{V}G - \bar{I}$ is suppressed.

The results obtained here are important in view of the interpretation of the experiment of Ref. 7. The observations of that experiment can also be explained if the observed dc voltage is the result of rectification of ac displacement currents generated by the time-dependent gate voltages that should drive the electron pump.²² Therefore, it is important to identify signatures that distinguish adiabatic pumping from mere rectification of displacement currents. For the case of a current measurement, two such signatures are the magnetic field symmetry and the typical size of the pumped current.^{10,22} Except for the case $N = 1$, our results allow to translate these signatures to a voltage measurement as well.²³ Further, the relation between pumped voltage and pumped current provides a third signature of an adiabatic pumping: For few-channel point contacts, \bar{I} , $\bar{V}G$, and the difference $\bar{V}G - \bar{I}$ are all random and of comparable magnitude for a quantum pump, while, if the dc signal is due to rectification, there is a fixed relationship $\bar{I} \propto G^2 \bar{V}$, the proportionality constant being non-universal.²²

We thank C. Marcus for discussions. This work was supported by the NSF under grant no. DMR-0086509 and by the Sloan foundation.

APPENDIX A:

Below we present results for the ‘‘intermediate’’ distributions of the normalized current \bar{i} , voltage \bar{v} , and of the difference $\bar{d} = \bar{v}g - \bar{i}$ after integration over the matrices Q_1 and Q_2 at fixed S and Q , but before integration over S and Q , for the case of a chaotic quantum dot with two single-channel point contacts. For that case, the distribution of \bar{d} is given by

$$P(\bar{d}) = \left\langle \frac{1}{2\sigma_d} e^{-|\bar{d}|/\sigma_d} \right\rangle_{S,Q}, \quad (\text{A1})$$

where the brackets $\langle \dots \rangle_{S,Q}$ denote the remaining average over the scattering matrix S and the symmetrized time-delay matrix Q . The distributions for \bar{i} , \bar{v} have the same form with σ_d replaced by σ_i and σ_v , respectively. However, we should note that, unlike for the difference \bar{d} , the form (A1) does not hold for the distributions of \bar{i} and \bar{v} when $N > 1$.

Below we list (statistical) expressions for σ_d , σ_i and σ_v for $N = 1$ for the case $C\Delta \ll e^2$. We introduce the eigenvalues τ_1, τ_2 of the normalized time-delay matrix R . Their distribution can be found in Ref. 18. Further, we introduce two independent random variables t (uniformly distributed between 0 and 1) and ϕ (uniformly distributed between 0 and 2π) that arise from the randomly distributed eigenvectors of R and the phases of the scattering matrix S . Finally, the equations for σ_d , σ_i , and σ_v contain the dimensionless conductance $g \in [0, 1]$, which has distribution $P(g) = (\beta/2)g^{-1+\beta/2}$. We then find

$$\begin{aligned} \sigma_{d,\beta=1}^2 &= 256 \frac{(\tau_1 \tau_2)^3}{(\tau_1 + \tau_2)^2} \frac{(1-g)^2}{g}, \\ \sigma_{i,\beta=1}^2 &= 256 \frac{(\tau_1 \tau_2)^3}{(\tau_1 + \tau_2)^2} g, \\ \sigma_{v,\beta=1}^2 &= 256 \frac{(\tau_1 \tau_2)^3}{(\tau_1 + \tau_2)^2} \frac{1}{g^3}, \\ \sigma_{d,\beta=2}^2 &= \frac{1-g}{g} \left(\frac{8\tau_1 \tau_2}{\tau_1 + \tau_2} \right)^2 \\ &\quad \times (\tau_1 \tau_2 + t(1-t)(\tau_1 - \tau_2)^2 \sin^2 \phi), \\ \sigma_{i,\beta=2}^2 &= (4\tau_1 \tau_2)^2 \left(1 - 4t(1-t) \left(\frac{\tau_1 - \tau_2}{\tau_1 + \tau_2} \right)^2 \right), \\ \sigma_{v,\beta=2}^2 &= \frac{1}{g^3} \left(\frac{8\tau_1 \tau_2}{\tau_1 + \tau_2} \right)^2 \left[\tau_1 \tau_2 + (\tau_1 - \tau_2)^2 \right. \\ &\quad \left. \times \left(2\sqrt{(1-g)t(1-t)} \sin \phi + (1-2t)\sqrt{g} \right)^2 \right]. \end{aligned}$$

¹ D. Thouless, Phys. Rev. B **27**, 6083 (1983).

² L. P. Kouwenhoven, A. T. Johnson, N. C. van der Vaart, C. J. P. M. Harmans, and C. T. Foxon, Phys. Rev. Lett. **67**, 1626 (1991).

³ H. Pothier, P. Lafarge, C. Urbina, D. Esteve, and M. H. Devoret, Europhys. Lett. **17**, 249 (1992).

⁴ T. H. Oosterkamp, L. P. Kouwenhoven, A. E. A. Koolen, N. C. van der Vaart, and C. J. P. M. Harmans, Phys. Rev. Lett. **78**, 1536 (1997).

⁵ For reviews, see L. P. Kouwenhoven *et al* in *Mesoscopic Electron Transport*, edited by L. L. Sohn, L. P. Kouwenhoven, and G. Schön (Kluwer, Dordrecht, 1997); C. W. J. Beenakker, Rev. Mod. Phys. **69**, 731 (1997); Y. Alhassid, Rev. Mod. Phys. **72**, 895 (2000).

⁶ B. Spivak, F. Zhou, and M. T. Beal Monod, Phys. Rev. B **51**, 13226 (1995).

⁷ M. Switkes, C. M. Marcus, K. Campman, and A. C. Gosard, Science **283**, 1905 (1999).

⁸ P. W. Brouwer, Phys. Rev. B **58**, 10135 (1998)

⁹ F. Zhou, B. Spivak, and B. Altshuler, Phys. Rev. Lett. **82**, 608 (1999).

¹⁰ T. A. Shutenko, I. L. Aleiner, and B. L. Altshuler Phys. Rev. B **61**, 10366 (2000).

¹¹ A. V. Andreev and A. Kamenev, Phys. Rev. Lett. **85**, 1294 (2000).

¹² I. L. Aleiner, B. L. Altshuler, and A. Kamenev, Phys. Rev. B **62**, 10373 (2000).

¹³ J. E. Avron, A. Elgart, G.M. Graf, and L. Sadun, Phys. Rev. B **62**, 10618 (2000).

¹⁴ M. Büttiker, A. Prêtre, and H. Thomas, Phys. Rev. Lett. **70**, 4114 (1993).

¹⁵ M. Büttiker, J. Phys. Condens. Matter **5**, 9361 (1993); M. Büttiker, H. Thomas, and A. Prêtre, Z. Phys. B **94**, 133 (1994).

¹⁶ Corrections to the self-consistent description are small as $1/N_{\text{ch}}$, where N_{ch} is the total number of channels connecting the dot to the reservoirs, including spin degeneracy, see I. L. Aleiner, P. W. Brouwer, and L. I. Glazman, to be published. Even for single-channel point contacts, one has $N_{\text{ch}} = 4$, and the quantitative effect of these corrections is small.

¹⁷ P. W. Brouwer, S. A. van Langen, K. M. Frahm, M. Büttiker, and C. W. J. Beenakker, Phys. Rev. Lett. **79**, 913 (1997).

¹⁸ P. W. Brouwer, K. M. Frahm, and C. W. J. Beenakker, Phys. Rev. Lett. **78**, 4737 (1997); *Waves in Random Media* **9**, 91 (1999).

¹⁹ The matrix $-i(\partial S/\partial E)S^\dagger = 2\pi R/\Delta$ is the Wigner-Smith time-delay matrix, see E. P. Wigner, Phys. Rev. **98**, 145 (1955), and F. T. Smith, Phys. Rev. **118**, 349 (1960).

²⁰ P. W. Brouwer and C. W. J. Beenakker, J. Math. Phys. **37**, 4904 (1996).

²¹ The tails of the distribution depend on the value of the capacitance C . In the non-interacting limit $C\Delta \gg e^2$ and $\eta = 0$, they read $P(\bar{d}) \propto \bar{d}^{-2}$ for $\beta = 1$ and $P(\bar{d}) \propto \bar{d}^{-3} \log \bar{d}$ for $\beta = 2$.

²² P. W. Brouwer, cond-mat/0012249.

²³ For single-channel contacts $N = 1$, \bar{v} is expressed in terms of the scattering matrix S as

$$\bar{v} = \frac{1}{(1+\eta)} \frac{2}{|S_{12}|^4} \text{Im} \left(\frac{\partial S_{11}}{\partial X_1} \frac{\partial S_{11}^*}{\partial X_2} - \eta \frac{\partial S_{22}}{\partial X_1} \frac{\partial S_{22}^*}{\partial X_2} \right).$$

Since $S(B) = S^T(-B)$ under reversal of a magnetic field B , this equation results in $\bar{v}(-B) = \bar{v}(B)$. There is no such magnetic field symmetry of the pumped voltage for $N > 1$.